Journal of Thrombosis and Haemostasis, **12**: 973–986 DOI: 10.1111/jth.12568

IN FOCUS

The Ca^{2+}/calmodulin-dependent kinase kinase β-AMP-activated protein kinase-α1 pathway regulates phosphorylation of cytoskeletal targets in thrombin-stimulated human platelets

M.-B. ONSELAER,* C. OURY,† R. W. HUNTER,‡ S. EECKHOUDT,§ N. BARILE,* C. LECUT,† N. MOREL,¶ B. VIOLLET,**††‡‡ L.-M. JACQUET,§§ L. BERTRAND,* K. SAKAMOTO,‡ J.-L. VANOVERSCHELDE,*¶¶ C. BEAULOYE*§§¶¶ and S. HORMAN*

**Institut de Recherche Expérimentale et Clinique (IREC), Pôle de Recherche Cardiovasculaire, Université catholique de Louvain, Brussels; †Human Genetics Unit, GIGA-Research, Laboratory of Thrombosis and Hemostasis, Université de Liège, Liège, Belgium; ‡Nestlé Institute of Health Sciences SA, Campus EPFL, Lausanne, Switzerland; §Department of Hematology, Cliniques universitaires Saint-Luc, Université catholique de Louvain; ¶Institute of Neuroscience, Laboratory of Cell Physiology, Université catholique de Louvain, Brussels, Belgium; **Institut Cochin, INSERM U1016; ††CNRS, UMR8104; ‡‡Université Paris Descartes, Sorbonne Paris Cité, Paris, France; §§Cliniques Universitaires Saint-Luc, Cardiovascular Intensive Care, Université catholique de Louvain; and ¶¶Division of Cardiology, Cliniques Universitaires Saint-Luc, Université catholique de Louvain, Brussels, Belgium*

To cite this article: Onselaer MB, Oury C, Hunter RW, Eeckhoudt S, Barile N, Lecut C, Morel N, Viollet B, Jacquet LM, Bertrand L, Sakamoto K, Vanoverschelde JL, Beauloye C, Horman S. The Ca^{2+}/calmodulin-dependent kinase kinase β-AMP-activated protein kinase-α1 pathway regulates phosphorylation of cytoskeletal targets in thrombin-stimulated human platelets. *J Thromb Haemost* 2014; **12**: 973–86.

See also Randriamboavonjy V, Fleming I. Energy and motion: AMPKa1 and its role in platelet activation. This issue, pp 970–2.

Summary. *Background:* Platelet activation requires sweeping morphologic changes, supported by contraction and remodeling of the platelet actin cytoskeleton. In various other cell types, AMP-activated protein kinase (AMPK) controls the phosphorylation state of cytoskeletal targets. *Objective:* To determine whether AMPK is activated during platelet aggregation and contributes to the control of cytoskeletal targets. *Results:* We found that AMPK-α1 was mainly activated by thrombin, and not by other platelet agonists, in purified human platelets. Thrombin activated AMPK-α1 *ex vivo* via a Ca^{2+}/calmodulin-dependent kinase kinase β (CaMKKβ)-dependent pathway. Pharmacologic inhibition of CaMKKβ blocked thrombin-induced platelet aggregation and counteracted thrombin-induced phosphorylation of several cytoskeletal proteins, namely, regulatory myosin light chains (MLCs), cofilin, and vasodilator-stimulated phosphoprotein (VASP), three key elements involved in actin cytoskeletal contraction and polymerization. Platelets isolated from mice lacking AMPK-α1 showed reduced aggregation in response to thrombin, and this was associated with defects in MLC, cofilin and VASP phosphorylation and actin polymerization. More importantly, we show, for the first time, that the AMPK pathway is activated in platelets of patients undergoing major cardiac surgery, in a heparin-sensitive manner. *Conclusion:* AMPK-α1 is activated by thrombin in human platelets. It controls the phosphorylation of key cytoskeletal targets and actin cytoskeletal remodeling during platelet aggregation.

Keywords: AMP-activated protein kinase; cytoskeleton; platelet aggregation; signal transduction; thrombin.

Correspondence: Christophe Beauloye, Avenue Hippocrate, 55 CARD5550, 1200 Brussels, Belgium.
Tel.: +32 2 764 5566; fax: +32 2 764 5536.
E-mail: christophe.beauloye@uclouvain.be

Received 23 September 2013
Manuscript handled by: S. Watson
Final decision: P. H. Reitsma, 11 March 2014

Introduction

Within seconds after activation, resting, discoid platelets are transformed into relatively spheroidal cells with filopodial extensions that are rapidly superseded by sustained lamellipodia characteristic of platelet spreading [1]. These morphologic changes are supported exclusively by contraction and remodeling of the platelet actin cytoskeleton [2,3]. Myosin IIA (encoded by the *MYH9* gene), the sole non-muscle myosin isoform present in platelets, interacts with actin to form contractile filaments. Its activity is regulated by reversible phosphorylation of

its regulatory myosin light chains (MLCs) on Thr18 or Ser19 [4]. MLC phosphorylation is critical for triggering platelet shape change and the centralization of secretory granules [2]. Centralization of granules may accelerate granule–granule fusion and connection to channels of the open canalicular system, to promote the secretion of granule products. Cofilin and vasodilator-stimulated phosphoprotein (VASP) are regulators of lamellipodia and filopodia, respectively [5,6]. Cofilin is a small, actin-dynamizing protein that regulates actin turnover in all species. Its phosphorylation at Ser3 inhibits its filamentous actin (F-actin) binding, severing and depolymerizing activities [5]. During secretion/aggregation, cofilin is characterized by cyclic dephosphorylation/phosphorylation behavior that promotes actin remodeling and the generation of free barbed ends for lamellipodium assembly during platelet activation. VASP is a regulator of actin polymerization. Its anticapping activity promotes filopodial formation, and contributes critically to the platelet aggregation response [7]. The localization and/or anticapping activity of the protein depend on its phosphorylation state [8]. Four main phosphorylation sites have been identified [8,9].

Ca^{2+}/calmodulin (CaM)-dependent kinase kinase β (CaMKKβ) is a CaM-binding protein whose activity is enhanced by thrombin in endothelial cells [10]. The serine/threonine kinase AMP-activated protein kinase (AMPK) has been identified as a substrate of CaMKKβ [11]. It is a heterotrimer consisting of a catalytic α-subunit (α1 or α2) and two regulatory subunits, β and γ. AMPK can be activated via an increase in Ca^{2+} concentration [10]. Acetyl-CoA carboxylase (ACC) is a genuine AMPK substrate, and its phosphorylation state is used to evaluate AMPK activation. In kidney epithelial cells, the CaMKKβ–AMPK-α1 pathway controls actin cytoskeletal contraction and organization via the indirect phosphorylation of MLCs and cofilin [12]. VASP has also been described as a direct substrate of AMPK [9,13].

As the CaMKKβ–AMPK-α1 pathway is a key factor in cytoskeletal organization, we hypothesized that it regulates platelet activation and aggregation by controlling the phosphorylation and activity of cytoskeletal proteins, namely MLCs, cofilin, and VASP. In this study, we established that thrombin activated the CaMKKβ–AMPK-α1 axis in human platelets. Pharmacologic or genetic inhibition of this pathway decreased platelet aggregation, modified MLC, VASP and cofilin phosphorylation states, and altered actin polymerization upon thrombin stimulation. Interestingly, the AMPK pathway was activated *in vivo* in platelets from patients undergoing major surgery.

Materials and methods

Materials are given in the supporting information (Part S1).

Approval of human and animal studies

Animal procedures and protocols were approved by local authorities (Comité d'éthique facultaire pour l'expérimentation animale, UCL/MD/2007/049 and 2012/UCL/MD/003) and performed in accordance with the Guide for the Care and Use of Laboratory Animals published by the US National Institutes of Health (NIH Publication No. 85-23, revised 1996). Human studies were authorized by the 'Commission d'Ethique Biomédicale Hospitalo-Facultaire de l'Université catholique de Louvain'. All human participants gave written, informed consent.

Platelet isolation and lysis

Human platelets Venous blood from healthy volunteers was collected in a 1 : 10 blood volume of 3.8% sodium citrate as anticoagulant (S-monovette). Platelet-rich plasma (PRP) was obtained by 15 min of centrifugation at 330 × *g*. For the measurement of intracellular Ca^{2+}, thromboxane A_2 (TXA_2) formation, platelet aggregation, secretion, and F-actin content, platelets were isolated from PRP by centrifugation at 800 × *g* in the presence of 0.1 μg mL^{-1} prostaglandin E_1 and 0.5 U mL^{-1} apyrase. The pellet was washed in modified Tyrode's buffer (135 mM NaCl, 12 mM $NaHCO_3$, 2.9 mM KCl, 0.3 mM Na_2HPO_4, 1 mM $MgCl_2$, 5 mM D-glucose, 10 mM Hepes, 0.35% bovine serum albumin [BSA], pH 7.4, 37 °C) containing 0.1 μg mL^{-1} prostaglandin E_1 and 0.5 U mL^{-1} apyrase. After centrifugation, platelets were resuspended to a density of 2.5 × 10^5 platelets μL^{-1} in modified Tyrode's buffer. For western blot analysis and immunoprecipitation experiments, platelets were purified from PRP in the presence of 4 μg mL^{-1} eptifibatide and 0.5 U mL^{-1} apyrase, with a density barrier of iodixanol (Optiprep Density Gradient Medium; Sigma-Aldrich, Diegem, Belgium), and resuspended to a density of 2.5 × 10^5 platelets μL^{-1} in modified Tyrode's buffer before treatment and lysis. For AMPK assays on immunoprecipitates and immunoblotting, extracts were prepared as previously described [14].

Murine platelets AMPK-α1 knockout (KO) mice were generated as previously described [15]. Males aged 8–12 weeks were bled under sodium pentobarbital anesthesia (25–35 mg kg^{-1}) from the retro-orbital plexus. Blood was collected in 1 : 6 acid–citrate–dextrose (ACD) solution with 1 U mL^{-1} apyrase. PRP was obtained by centrifugation at 800 × *g* for 5 s, followed by 5 min at 100 × *g*. PRP from three mice was pooled and washed by adding two volumes of ACD. Platelets were pelleted for 10 min at 800 × *g*, and resuspended to a density of 2.5 × 10^5 platelets μL^{-1} in modified Tyrode's buffer for the measurement of platelet aggregation, activation, and F-actin content, and for western blot analysis and immunoprecipitation experiments. At least three independent experiments were performed on washed platelets from different pools.

Measurement of platelet aggregation and ATP secretion analyses

Light transmission during thrombin-induced aggregation in washed human and murine platelets was recorded at 37 °C, with constant stirring (1200 r.p.m.), in an aggregometer (Chrono-Log Stago, Leiden, The Netherlands). ATP secretion was monitored in washed platelets in parallel with platelet aggregation by adding firefly luciferase and luciferin and comparing the luminescence generated by platelet ATP release with an ATP standard (Chrono-Lume; Stago, Leiden, The Netherlands). At least three independent experiments were performed on platelets from different individuals.

Detection of CD62P and PAC1/JON/A by flow cytometry, western blotting, cytosolic Ca^{2+} measurement, measurement of thromboxane B_2 (TXB_2) formation, and quantitation of F-actin

Please see the supporting information Part S1.

Enzyme assays

AMPK activity was measured as previously described after immunoprecipitation of 50 μg of platelet extracts with 10 μg of AMPK-α1 or AMPK-α2 antibodies [14].

Liver kinase B1 (LKB1) was immunoprecipitated from platelet lysate protein (1 mg) incubated at 4 °C for 1 h on a shaking platform with 5 μL of protein G–Sepharose covalently conjugated to 2 μg of human LKB1 antibody or preimmune IgG. LKB1 activity was measured with LKBtide, as previously described [16].

Microscopic analysis of platelet spreading

Glass coverslips were coated overnight with fibrinogen (100 μg mL^{-1}), and this was followed by surface blocking with BSA (5 mg mL^{-1} in phosphate-buffered saline [PBS]). Washed platelets in Hepes/Tyrode buffer (20×10^3 platelets μL^{-1}) were stimulated or not stimulated with thrombin (0.05 U mL^{-1}) in the presence of $CaCl_2$ (2 mM) just before being exposed to the surface at 37 °C. After 1 h, non-adherent platelets were discarded, and surface-bound platelets were washed three times with PBS. Coverslips were fixed in 4% paraformaldehyde, washed with PBS, and permeabilized with blocking buffer (PBS, 0.1% SDS + 1% BSA) containing tetramethylrhodamine isothiocyanate–phalloidin (1 : 100) for 1 h in the dark. Coverslips were mounted with Fluoromount G (SouthernBiotech, Birmingham, AL, USA) on glass slides, and visualized with a Zeiss (× 100 oil immersion) fluorescent microscope (Carl Zeiss, Zaventem, Belgium) equipped with ApoTome (Axio Imager).

Clot retraction assay

PRP (adjusted to 6×10^5 platelets μL^{-1} for murine platelets, 300 μL) was obtained by centrifugation of whole blood at 800 × *g* for 5 s, followed by 5 min at 100 × *g*. Clot formation was initiated by the addition of 300 μL of a solution containing thrombin (1 U mL^{-1}, final concentration) in the the presence of $CaCl_2$ (2 mM, final concentration). The clots were allowed to retract for up to 1 h at 37 °C, and were photographed at different time points. The extent of retraction was quantified by the Image J program (Version 1.440; National Institutes of Health, Bethesda, MD, USA), and retraction was expressed as a percentage ([final clot size/initial clot size] × 100).

Study population

Six consecutive patients scheduled for elective cardiopulmonary bypass (CPB) surgery were recruited. None of them received antiplatelet agents for at least 5 days before surgery. Patients who had suffered from acute coronary syndrome or another thrombotic process in a period of 6 months before surgery were also excluded. A first blood sample was drawn during CPB surgery, after bolus administration of unfractionated heparin (UFH) (to achieve an activated clotting time [ACT] of > 450 s). A second blood sample was taken 4 h after surgery in the intensive care unit (ICU) and after blood coagulation correction. Thrombin time (TT) (Thromboclotin; Siemens, Saint-Denis, France) and activated partial thromboplastin time (APPT) (Platelin L; bioMérieux, Craponne, France) were measured in a tube containing 0.129 M trisodium citrate in a coagulation device (MDA 2; bioMérieux).

In addition, multiplate analysis was performed in the postoperative setting (4 h) to exclude patients showing platelet dysfunction after CBP surgery.

Statistics

The mean and standard error of the mean were calculated for all experimental groups. The significance of differences between the mean values of different groups was determined with GRAPHPAD PRISM (GraphPad Software, La Jolla, CA, USA), by the use of a two-tailed unpaired Student's test and analysis of variance (ANOVA), as appropriate. $P < 0.05$ was considered to be significant.

Results

CaMKKβ-dependent AMPK-α1 activation is induced by thrombin in human platelets

AMPK-α1, but not AMPK-α2, was detected in purified human platelets (Fig. 1A). AMPK-α1 was activated threefold upon stimulation with 0.1 U mL^{-1} thrombin (Fig. 1B). AMPK-α1 activation resulted in increased phosphorylation on Ser79 of ACC, the downstream substrate of AMPK (Fig. 1C). Dose–response curves for activating peptides for protease-activated receptor (PAR)1 (PAR1-

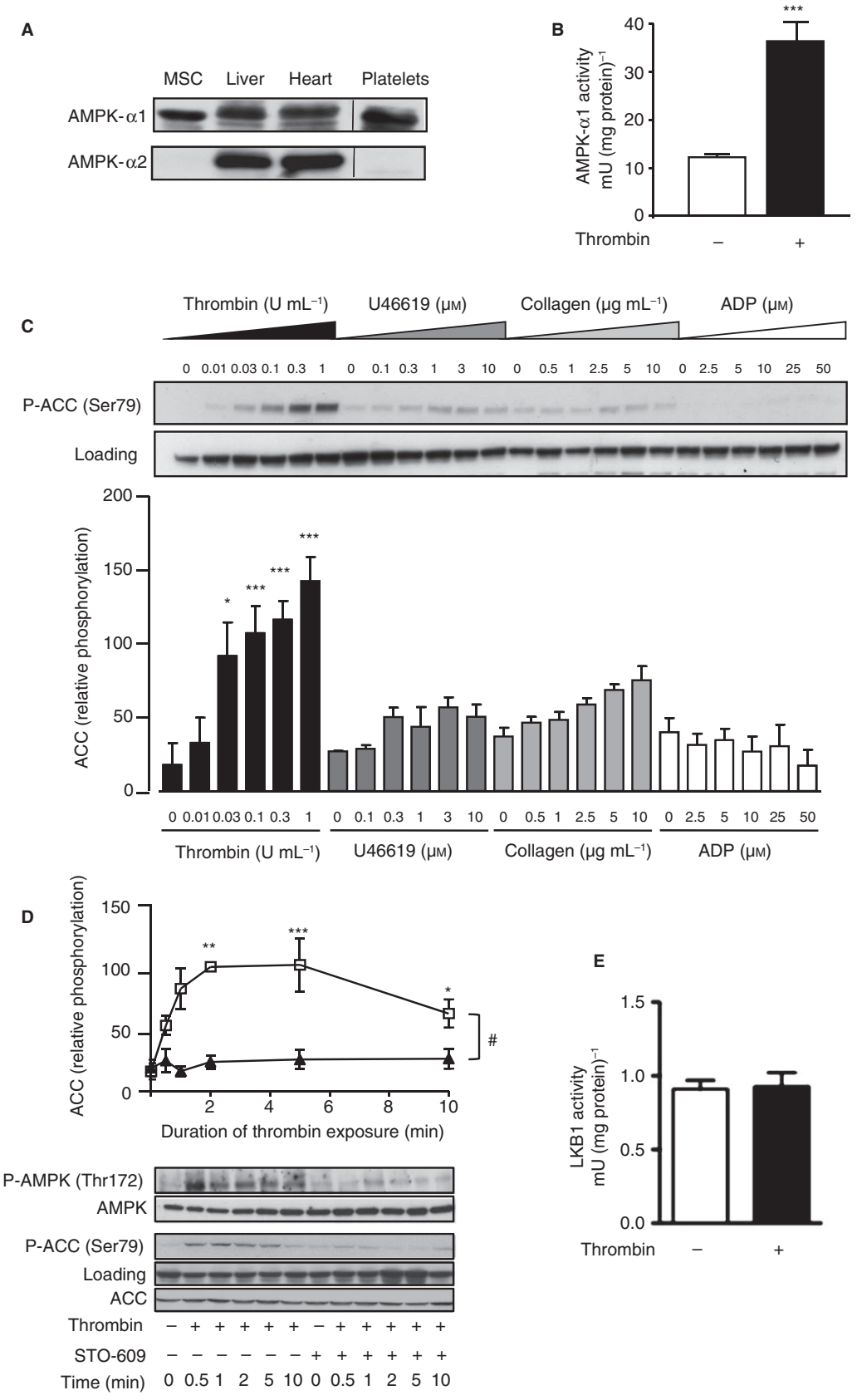

Fig. 1. Thrombin-induced AMP-activated protein kinase (AMPK)-α1 activation in human platelets. (A) Western blot analysis of AMPK-α1 and AMPK-α2 expression in extracts of mouse mesenchymal stem cells (MSCs), rat liver, rat heart, and human platelets. MSC (AMPK-α1 expression) and liver and heart (AMPK-α1 and AMPK-α2 expression) served as positive controls. A solid line is included to denote that samples were run on the same gel but were not contiguous. (B) Purified platelets were incubated with 0.1 U mL^{-1} thrombin for 1 min prior to cell lysis. Platelet lysates were immunoprecipitated with anti-AMPK-α1 antibody for AMPK assays. The data are expressed as mean ± standard error of the mean (SEM) of four independent experiments. ***$P < 0.001$ as compared with controls without thrombin. (C) Acetyl-CoA carboxylase (ACC) phosphorylation in purified human platelets incubated with increasing doses of thrombin, U46619, collagen and ADP for 2 min prior to cell lysis. A representative blot is shown in the upper panel, and data quantification for phospho-ACC (P-ACC) is shown in the lower panel. The results are the mean ± SEM of three separate experiments. *$P < 0.05$ and ***$P < 0.001$ as compared with corresponding control values. (D) ACC phosphorylation in purified platelets incubated in the presence (▲) or absence (□) of 10 μM STO-609 for 2 min prior to stimulation with 0.1 U mL^{-1} thrombin for the indicated times. Representative blots of phospho-AMPK (P-AMPK) and P-ACC are shown in the lower panel, and data quantification for P-ACC is shown in the upper panel. The data are expressed as mean ± SEM, $n = 7$. *$P < 0.05$, **$P < 0.01$ and ***$P < 0.001$ as compared with corresponding control values; $^{\#}P < 0.05$ represents a statistical difference between the treatment with thrombin in the presence (▲) and absence (□) of STO-609). (E) Liver kinase B1 (LKB1) activity was determined in anti-LKB1 immune complexes isolated from 1 mg of platelet lysate after stimulation with 0.1 U mL^{-1} thrombin for 1 min prior to cell lysis. The data are expressed as mean ± SEM of three independent experiments.

AP) and for PAR4 (PAR4-AP) showed that maximal ACC phosphorylation was observed at concentrations of 0.3 μM PAR1-AP and 300 μM PAR4-AP, confirming that PAR1 is the main mediator of thrombin-induced signaling in human platelets (Fig. S1). Other platelet agonists – U46619, a potent and stable TXA_2 receptor agonist, collagen, and ADP – barely affected ACC phosphorylation as compared with thrombin (Fig. 1C). CaMKKβ, an upstream kinase of AMPK, is an obvious candidate for mediating thrombin-induced AMPK activation in platelets. In human platelet extracts, anti-CaMKKβ antibody recognized two bands at ~ *65 kDa,* probably corresponding to distinct isoforms encoded by splice variants (Fig. S2A). Moreover, the presence of this AMPK kinase in platelets is supported by the study of Rowley *et al*. [17] on mouse and human platelet transcriptomes. STO-609 (10 μM), a selective CaMKKβ inhibitor, completely blocked AMPK activation by thrombin, as demonstrated by reduced AMPK and ACC phosphorylation on Thr172 and Ser79, respectively (Fig. 1D). In contrast, STO-609 did not prevent ACC phosphorylation when platelets were treated with A-769662, a specific pharmacologic activator of AMPK, making a direct inhibitory effect of STO-609 on AMPK unlikely (Fig. S2B). LKB1, the other AMPK kinase, was not activated in response to thrombin (Fig. 1E), and therefore cannot be responsible for the thrombin-induced AMPK activation and the subsequent ACC phosphorylation.

CaMKKβ-dependent platelet aggregation is induced by thrombin in human platelets

STO-609 inhibited thrombin-induced platelet aggregation (Fig. 2A,B) but did not affect aggregation induced by low concentrations of U46619 (0.3 and 1 μM), collagen (2.5 and 5 μg mL^{-1}), or ADP (2.5 and 10 μM) (Fig. S3). It also significantly suppressed PAC-1 binding in response to thrombin (Fig. 2C), indicating reduced activation of $\alpha_{IIb}\beta_3$ integrin on the platelet surface. This might be attributable to a reduction in secretion. Therefore, α-granule and dense granule release were evaluated by measuring P-selectin (CD62P) on the platelet surface and ATP secretion, respectively. STO-609 significantly inhibited CD62P exposure on platelets and ATP secretion after stimulation with thrombin (Fig. 2D,E), but not in response to other agonists (Fig. S3). This inhibitory effect did not result from an alteration of Ca^{2+} signaling. Indeed, this compound did not modify the increase in Ca^{2+} concentration in response to thrombin (Fig. S4A). Moreover, STO-609 did not affect thrombin-induced TXB_2 production (Fig. S4B).

CaMKKβ-dependent phosphorylation of MLCs, VASP and cofilin in human platelets is stimulated by thrombin

The CaMKKβ–AMPK-α1 pathway tightly regulates actin cytoskeletal contraction and organization. The latter is crucial for platelet aggregation. Accordingly, the phosphorylation state of cytoskeletal targets downstream of CaMKKβ–AMPK, namely, MLCs, cofilin, and VASP, was studied after stimulation with thrombin. MLC phosphorylation on Ser19 was detected at 30 s, and reached a maximum 2 min after thrombin addition (Fig. 3A). STO-609 significantly reduced MLC Ser19 phosphorylation (Fig. 3A). In endothelial cells treated with thrombin, AMPK controls VASP by phosphorylating Thr278 [13]. In purified human thrombin-stimulated platelets, VASP Thr278 phosphorylation increased transiently from 30 s until 2 min, and returned to control values after 10 min (Fig. 3B). This phosphorylation was significantly reduced in the presence of STO-609 (Fig. 3B). Finally, Fig. 3C shows that thrombin led to increased cofilin phosphorylation on Ser3, which persisted for 10 min. A decrease in cofilin phosphorylation was observed in the presence of STO-609 (Fig. 3C). Taken together, these findings show that the phosphorylation state of cytoskeletal targets was clearly affected by pharmacologic inhibition of CaMKKβ–AMPK-α1.

Actin cytoskeletal rearrangements upon thrombin stimulation include actin polymerization. To investigate the influence of CaMKKβ on actin polymerization, we measured the F-actin/free globular actin ratio in platelets

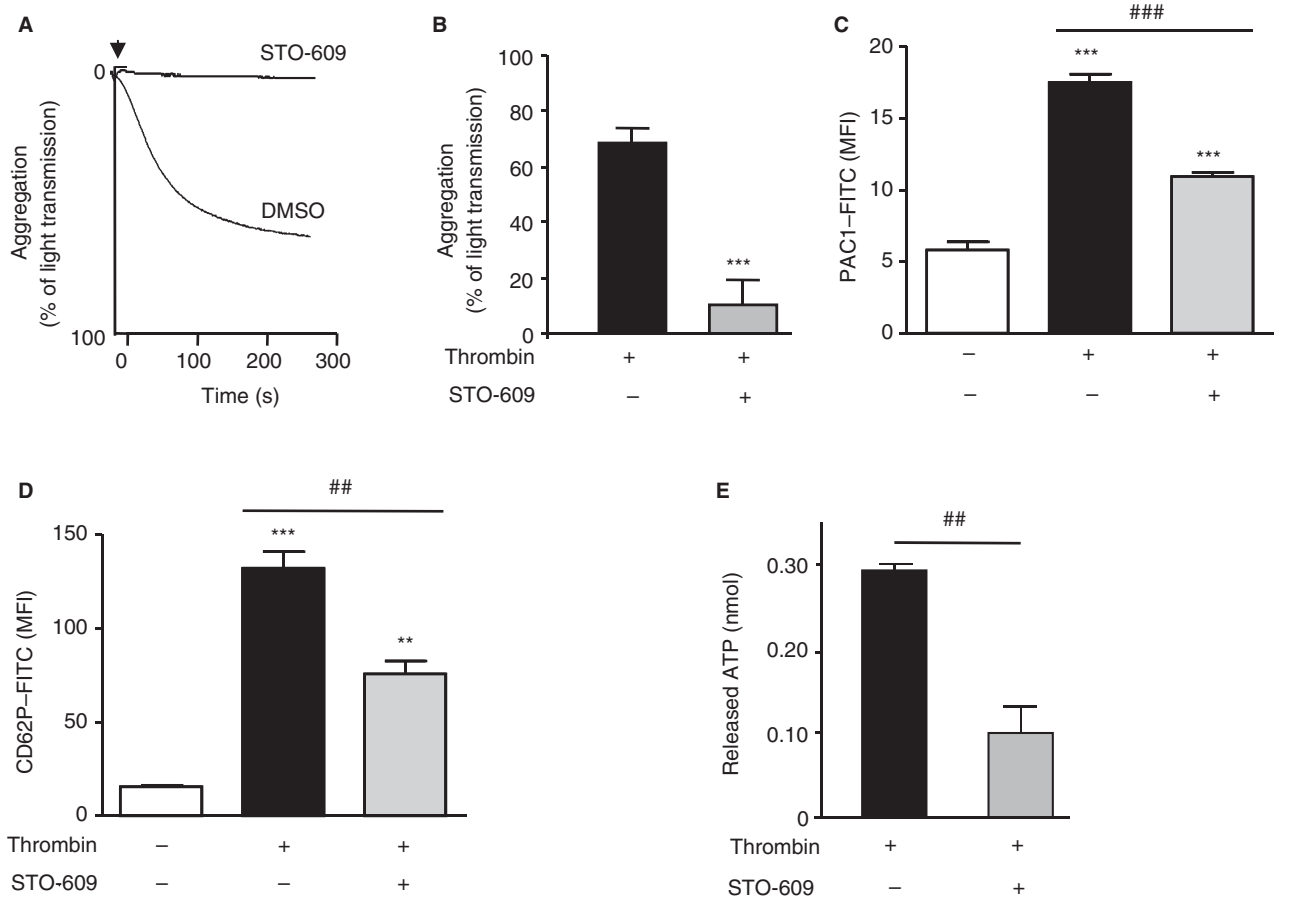

Fig. 2. The Ca^{2+}/calmodulin-dependent kinase kinase β-AMP-activated protein kinase-α1 pathway regulates thrombin-induced human platelet aggregation and secretion. (A) Washed platelets were incubated for 2 min with 10 μM STO-609, prior to thrombin stimulation (0.03 U mL^{-1}). Percentage of light transmission was measured by aggregometry (Chrono-Log). (B) Quantification of data from 10 independent experiments, expressed as mean ± standard error of the mean (SEM). ***$P < 0.001$ as compared with corresponding control values. (C–E) Effect of STO-609 on thrombin-induced $\alpha_{IIb}\beta_3$ activation (C), α-granule secretion (D), and ATP secretion (E). Washed platelets were incubated with 10 μM STO-609 for 2 min prior to stimulation with 0.03 U mL^{-1} thrombin. The results are the mean ± SEM, $n = 5$. **$P < 0.01$ and ***$P < 0.001$ as compared with corresponding control values; $^{\#\#}P < 0.01$ and $^{\#\#\#}P < 0.001$ represent a statistical difference between the treatment with thrombin in the presence and absence of STO-609. DMSO, dimethylsulfoxide; FITC, fluorescein isothiocyanate; MFI, mean fluorescence units.

treated with thrombin in the presence or absence of STO-609. Figure 3D shows that inhibition of CaMKKβ prevented the increase in F-actin induced by thrombin stimulation. These results were confirmed by detecting F-actin with flow cytometry (Fig. 3E).

Reduced aggregation of AMPK-α1-deficient murine platelets

Both catalytic subunits of AMPK, namely AMPK-α1 and AMPK-α2, are expressed in murine platelets, as described previously [18] (Fig. 4A). ACC was phosphorylated upon

Fig. 3. The Ca^{2+}/calmodulin-dependent kinase kinase β-AMP-activated protein kinase-α1 pathway contributes to thrombin-induced phosphorylation of cytoskeletal proteins and actin polymerization in human platelets. Purified platelets were incubated with 0.1 U mL^{-1} thrombin in the presence (▲) or absence (□) of 10 μM STO-609, and lysates were harvested for western blotting. (A–C) Representative blots showing myosin light chain (MLC) (A), vasodilator-stimulated phosphoprotein (VASP) (B) and cofilin (C) phosphorylation states are shown in the left panels. Quantitative results are shown in the right panels. The data are mean ± standard error of the mean (SEM), $n = 6$. *$P < 0.05$, **$P < 0.01$ and ***$P < 0.001$ as compared with corresponding control values. $^{\#}P < 0.05$ and $^{\#\#}P < 0.01$ represent a statistical difference between the treatment with thrombin in the presence and absence of STO-609). (D) Globular actin and filamentous actin (F-actin) were detected with actin antibody, and the percentage of F-actin was quantified. Bars represent mean ± SEM, $n = 4$. **$P < 0.01$ as compared with corresponding control values. $^{\#\#}P < 0.01$ represents a statistical difference between the treatment with thrombin in the presence and absence of STO-609). (E) Platelets were stained with 10 μM fluorescein isothiocyanate (FITC)–phalloidin and and analyzed with flow cytometry. Data are expressed as percentage of control of resting platelets that were incubated with vehicle alone. Bars represent mean ± SEM, $n = 4$. *$P < 0.05$ as compared with corresponding control values. $^{\#}P < 0.05$ represents a statistical difference between the treatment with thrombin in the presence and absence of STO-609). P-cofilin, phospho-cofilin; P-MLC, phospho-MLC; P-VASP, phospho-VASP.

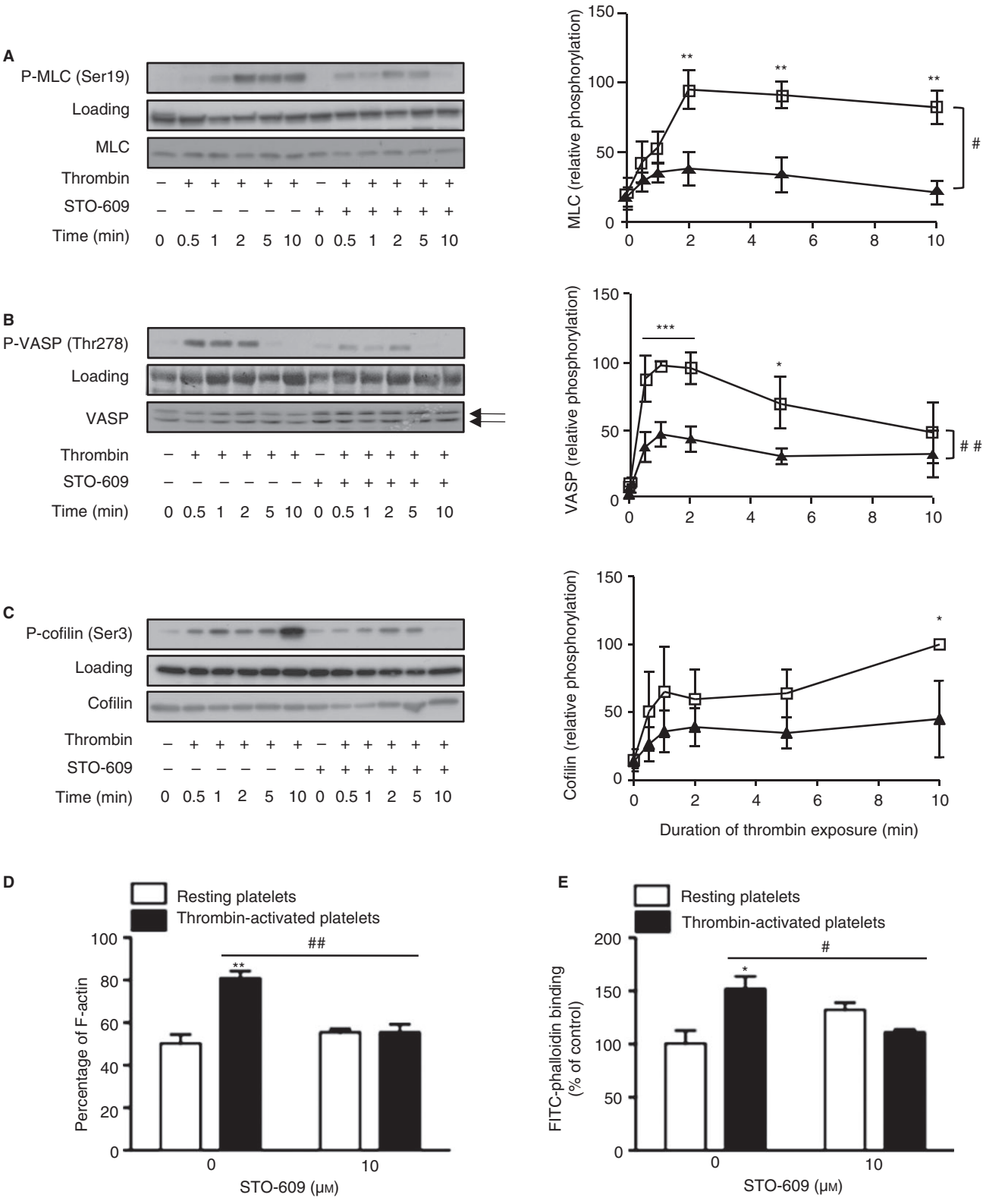

thrombin stimulation (Fig. 4B). In contrast to what was seen in human platelets, thrombin, TXA_2 and collagen led to similar levels of ACC phosphorylation (Fig. 4C). The isoform's contribution to AMPK activation of thrombin-stimulated murine platelets was determined by measuring ACC phosphorylation in platelets from AMPK-α1 KO and AMPK-α2 KO mice as compared with their wild-type (WT) littermates. AMPK-α1 made a major contribution to mediating ACC phosphorylation in response to thrombin and to other platelet agonists as

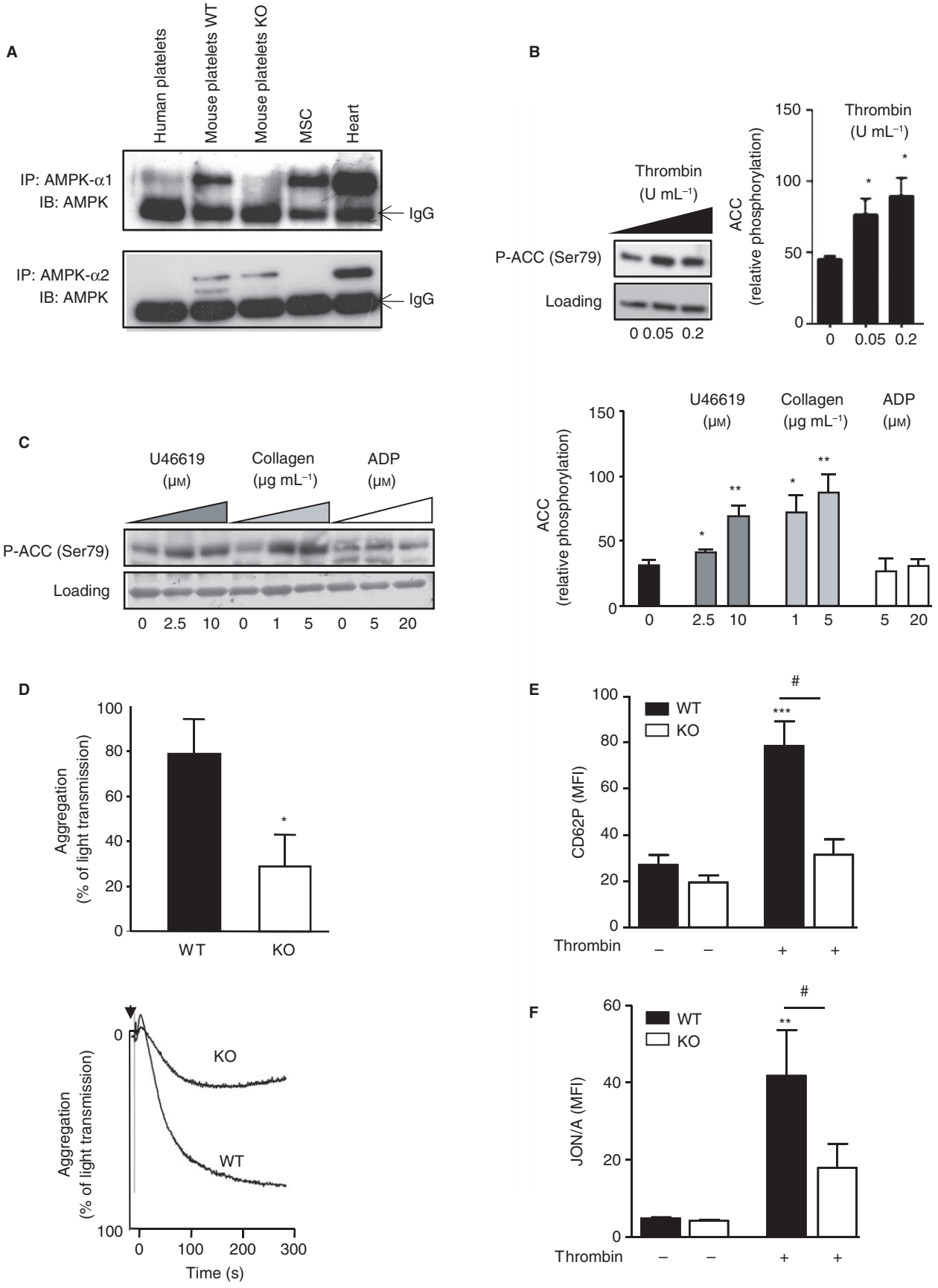

Fig. 4. Role of AMP-activated protein kinase (AMPK)-α1 in murine platelet aggregation and secretion. (A) Platelet lysates from wild-type (WT) and AMPK-α1 knockout (KO) mice were immunoprecipitated with anti-AMPK-α1 and anti-AMPK-α2 antibodies, and analyzed by western blotting with total anti-AMPK antibody. Human platelets, mouse mesenchymal stem cells (MSCs) and rat heart extracts were positive controls for the detection of AMPK-α1 and AMPK-α2, respectively. (B, C) Washed murine platelets were incubated with increasing doses of (B) thrombin (0.05; 0.2 U mL^{-1}) or (C) U46619 (2.5; 10 μM), collagen (1; 5 μg mL^{-1}) and ADP (5; 20 μM) for 2 min prior to cell lysis and western blot analysis for acetyl-CoA carboxylase (ACC) phosphorylated on Ser79. Representative blots are shown in the left panel, and data quantification for phospho-ACC (P-ACC) is shown in the right panel. The results are the mean ± standard error of the mean (SEM)of six separate experiments. $*P < 0.05$ as compared with control values. (C) Washed platelets were stimulated with thrombin (0.05 U mL^{-1}) before measurement of aggregation. A representative aggregation tracing is shown in the lower panel. The results are represented as mean ± SEM, $n = 4$. $*P < 0.05$ as compared with the WT value. (D, E) α-Granule secretion (D) and $\alpha_{IIb}\beta_3$ activation (E). Washed platelets were incubated for 5 min with thrombin (0.05 U mL^{-1}) before analysis with flow cytometry. Quantification of the respective data is presented as mean ± SEM, $n = 5$. $**P < 0.01$ and $***P < 0.001$ as compared with control WT values. $^{\#}P < 0.05$ represents a statistical difference between platelets from WT and AMPK-α1 KO mice treated with thrombin. IB, immunoblotting; IP, immunoprecipitation.

compared with AMPK-α2 (Fig. S5). On the basis of this observation and on our demonstration that AMPK-α1 accounted for all of the AMPK in human platelets, we measured thrombin-induced platelet aggregation and secretion in AMPK-α1 KO mice. At 0.05 U mL^{-1} thrombin, platelets from KO mice had a clear aggregation defect, implicating the α1 catalytic subunit in platelet function (Fig. 4D). AMPK-α1 deficiency inhibited platelet secretion after thrombin stimulation (Fig. 4E) and reduced the amount of activated $\alpha_{IIb}\beta_3$ (Fig. 4F). A slight aggregation defect was detected upon U46619 and collagen stimulation in platelets from AMPK-α1 KO mice (Fig. S6A,B), and was associated with a decrease in ATP secretion (Fig. S6C). However, after stimulation with 5 μM U46619 and 2.5 μg mL^{-1} collagen, α-granule secretion and subsequent P-selectin exposure on the platelet surface were not sufficiently increased under static conditions for a difference between WT and KO platelets to be detected (Fig. S6D).

Regulation of MLC, VASP and cofilin phosphorylation by AMPK-α1 and its impact on actin polymerization in thrombin-stimulated murine platelets

The experiment illustrated in Fig. 5A shows that the increase in thrombin-induced ACC phosphorylation was reduced by ~ 75% in platelets from AMPK-α1 KO mice as compared with those from WT mice, meaning that the residual phosphorylation resulted from AMPK-α2 activation. Altered function of platelets isolated from KO mice was associated with changes in MLC, VASP and/or cofilin phosphorylation. As in human platelets, 0.05 U mL^{-1} thrombin induced increases in MLC, VASP and cofilin phosphorylation in mouse platelets. The phosphorylation was significantly reduced in platelets from AMPK-α1 KO littermates (Fig. 5B–D), and was associated with abrogation of thrombin-dependent F-actin formation, as demonstrated by flow cytometry (Fig. S7). Platelet spreading and fibrin clot retraction are both dependent on the actin cytoskeleton. We therefore examined the mean area covered by the adhering platelets and the formation of filopodia and lamellipodia after immobilization on fibrinogen-coated coverslips and stimulation with thrombin for 60 min. Whereas the surface areas of the spread WT and KO platelets were similar at this time point, the percentage of platelets able to form lamellipodia was significantly reduced in the absence of AMPK-α1 (Fig. 5E–G), indicating altered cytoskeletal reorganization in spread KO platelets. More importantly, clot retraction was slower and less effective in KO platelets (Fig. 5H).

In vivo *activation of the AMPK pathway by thrombin in human platelets from patients undergoing major surgery*

In order to determine whether the AMPK pathway was also activated *in vivo* by thrombin, we studied ACC phosphorylation in platelets from patients undergoing major cardiac surgery. Under these conditions, the coagulation cascade is fully activated. During cardiac surgery, patients were subjected to CPB requiring heparin administration to block thrombin generation. This gave us a unique opportunity to assess ACC phosphorylation in the same patients, under two extreme conditions, in terms of thrombin generation: CPB (in the presence of heparin), and postsurgery in the ICU (normal coagulation). During CPB, the mean ACT was 568 ± 65 s, and the APTT and TT were over 180 s and 120 s, respectively. The ability to coagulate was restored 4 h after surgery (APTT, 30 ± 2 s; TT, 25 ± 3 s). The International Normalized Ratio and fibrinogen level were normal (not shown), and the platelet count was > 10^5 mm^{-3} for each patient. ACC phosphorylation increased significantly postsurgery (with normal coagulation) as compared with during CPB (under high-dose UFH) (Fig. 6A,B).

Discussion

With pharmacologic and genetic approaches, our study demonstrates that inhibition of the CaMKKβ–AMPK-α1 pathway in both mice and humans is associated with altered platelet aggregation in response to thrombin.

This pathway controls the phosphorylation of cytoskeletal targets and actin polymerization, which are known to be crucial in platelet contraction and shape change. More importantly, we show, for the first time, that the AMPK pathway is activated in human platelets.

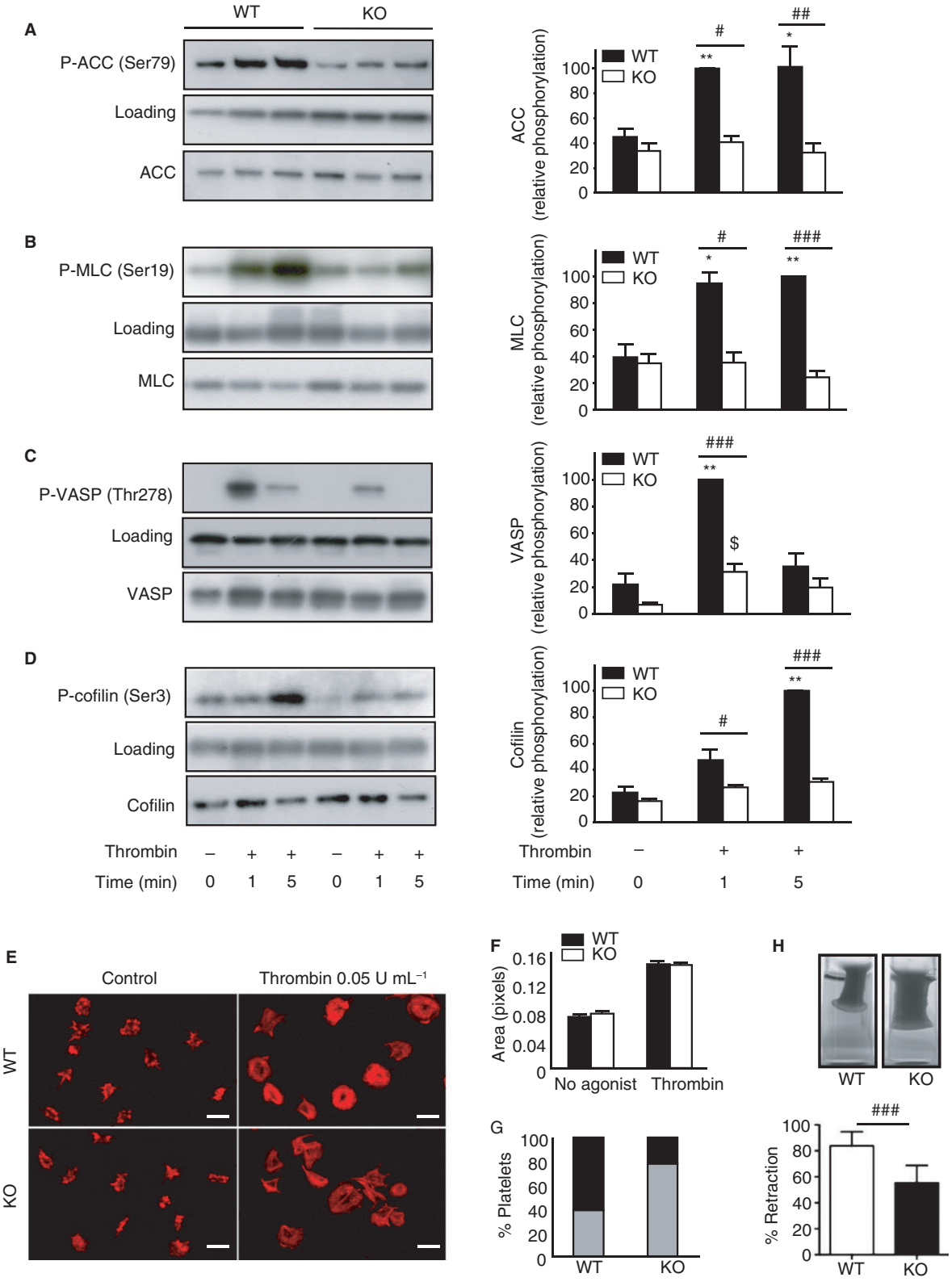

In human platelets, PAR1 and PAR4 mediate most of the response to thrombin. However, the concentration of PAR4-AP necessary to induce ACC phosphorylation was 300-fold higher than that of PAR1-AP (Fig. S1), confirming that PAR1 is the main receptor for thrombin in human platelets. In contrast, mouse platelets express PAR3 and PAR4. Activation of mouse platelets by thrombin completely depends on PAR4, as demonstrated

Fig. 5. The AMP-activated protein kinase-α1 pathway contributes to thrombin-induced phosphorylation of cytoskeletal proteins, actin polymerization, spreading and clot retraction in murine platelets. (A–D) Washed platelets were incubated with 0.05 U mL^{-1} thrombin for the indicated times. Representative blots of phospho-acetyl-CoA carboxylase (P-ACC) (A), phospho-myosin light chain (P-MLC) (B), phospho-vasodilator-stimulated phosphoprotein (P-VASP) (C) and phospho-cofilin (P)-cofilin (D) are shown in the left panels. Quantitative results are plotted in histograms (right panels). The data are mean ± standard error of the mean (SEM), $n = 5$. $^{*}P < 0.05$ and $^{**}P < 0.01$ as compared with control wild-type (WT) values. $^{\$}P < 0.05$ as compared with control knockout (KO) values. $^{\#}P < 0.05$, $^{\#\#}P < 0.01$ and $^{\#\#\#}P < 0.001$ represent a statistical difference between platelets from WT and AMPK-α1 KO mice treated with thrombin. (E–G) Washed platelets were plated on fibrinogen-coated coverslips for 60 min, in the presence or absence of 0.05 U mL^{-1} thrombin. (E) Cells were fixed, permeabilized, and stained with rhodamine–phalloidin to visualize actin. Scale bar: 5 μm. (F) Quantification of platelet surface area outlined by computer analysis. (G) The percentage of platelets showing lamellipodia (black bar) and/or filopodia (gray bar). Histograms represent the mean values from 250 platelets. (H) Clot retraction assessed at 1 h after addition of thrombin. The images in upper panel show a representative result. Data are presented as mean ± SEM, $n = 3$. $^{\#\#\#}P < 0.001$ represents a statistical difference between platelets from WT and AMPK-α1 KO mice treated with thrombin.

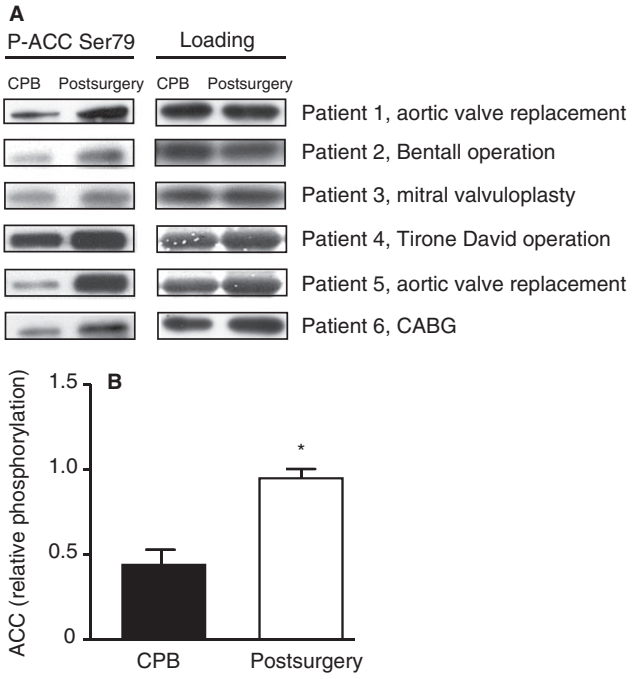

Fig. 6. Clinical evidence of AMP-activated protein kinase activation in human platelets after major cardiac surgery. Blood samples were drawn from six patients during cardiopulmonary bypass (CPB) surgery and 4 h after surgery. Human platelet lysates were analyzed by western blotting with antibody against phospho-acetyl-CoA carboxylase (P-ACC) (Ser79) (A) and quantified by densitometry after normalization to glyceraldehyde-3-phosphate dehydrogenase expression (B). The data are expressed as mean ± standard error of the mean, $n = 6$. $^{*}P < 0.05$ as compared with CPB values. CABG, coronary artery bypass graft.

by the absence of response to thrombin of platelets from *PAR4 KO* mice, despite the presence of PAR3 [19]. This could explain, at least in part, the different responses to agonists in human and mouse platelets.

The hypothesis that AMPK is involved in platelet function has been advanced in a previous study [18]. The authors reported that AMPK-α2 appears to be more important than AMPK-α1 in the regulation of platelet function. We cannot exclude the possibility that both AMPK catalytic isoforms control platelet aggregation in mice by acting on different targets. However, only AMPK-α1 was detected in highly purified human platelets according to the Optiprep protocol. More importantly, our finding is strongly supported by Rowley, who identified both conserved and differential expression patterns in human and mouse platelet transcriptomes [17]. This study indicates that the gene encoding AMPK-α2, *PRKAA2*, belongs to the list of genes expressed in mouse platelet samples, but is not expressed in human platelets. We have thus confirmed that AMPK-α2 is not present in human platelets. This observation supports the concept that signaling events taking place in mouse platelets can diverge from those in human platelets.

LKB1 was proposed to be the main AMPK kinase in platelets [18]. Phosphorylation on Thr189 was indeed increased upon thrombin stimulation. However, LKB1 is a constitutively active kinase whose activity is set in cells by the relative levels of its two partners, STRAD and MO25 [16]. We measured LKB1 activity after coimmunoprecipitation of the enzymatic complex from platelet extracts. Our data show that there is no LKB1 activation after thrombin stimulation. Therefore, we used the STO-609 inhibitor to demonstrate that CaMKKβ is the main AMPK kinase involved in AMPK activation in this condition. Several studies on platelet signaling have shown that short preincubation periods (60 s to 5 min) are mostly sufficient for maximal inhibition of kinases by pharmacologic inhibitors [20,21]. Indeed, a 2-min preincubation with 10 μM STO-609 completely blocked the thrombin-induced ACC phosphorylation and platelet aggregation. Again, these data are in disagreement with those of Randriamboavonjy *et al.* [18], who showed that STO-609 even tended to potentiate the thrombin-induced aggregation of human platelets. However, the duration of preincubation with the inhibitor before thrombin stimulation differed between our respective studies (2 min vs. 30 min). We have verified that a 30-min period of preincubation with STO-609 does not inhibit platelet aggregation (data not shown).

It was surprising to find that AMPK-α1 was mainly activated downstream of thrombin in human platelets, whereas the other agonists also induced an increase in the cytosolic Ca^{2+} concentration. Although the Ca^{2+} level is obviously a determinant factor for CaMKKβ activation, there should be additional Ca^{2+}-independent mechanisms involved in its regulation. In this respect, Green *et al.* [22]

recently reported a novel type of regulation of CaMKKβ activity, i.e. by multisite phosphorylation. Further investigations should therefore consider the phosphorylation status of this AMPK kinase, in order to obtain a better understanding of its regulation in response to the different platelet agonists, and particularly in response to thrombin, in addition to the classic CaM binding.

We have already reported that the CaMKKβ–AMPK-α1 pathway triggers actin cytoskeletal remodeling in epithelial cells via indirect MLC and cofilin phosphorylation [12]. In platelets, RhoA signaling causes MLC phosphorylation. The molecular mechanism involves phosphorylation and inhibition of myosin phosphatase-targeting subunit-1 (MYPT1) by Rho kinase [23]. It is tempting to speculate that AMPK could indirectly regulate MLC phosphorylation in platelets by stimulating RhoA or via direct inhibition of MYPT1, a protein from the PPP1R12 family of protein phosphatase regulatory subunits. The latter hypothesis is supported by the work of Banko *et al*. [24], who identified MYPT1 and MBS85 as direct *in vivo* substrates of AMPK. In the same study, p21-activated protein kinase 2 (PAK2) was also described as a direct substrate of AMPK that is able to regulate MLC phosphorylation. The involvement of MBS85/MYPT1 and PAK2 in AMPK-dependent MLC phosphorylation in thrombin-treated platelets remains to be elucidated.

Besides RhoA, Ca^{2+}-dependent Rac1 activation has been implicated in regulating aggregation in human platelets treated with thrombin, notably by stimulating rapid cofilin dephosphorylation/activation through a cofilin phosphatase [5,25]. This rapid first phase of cofilin dephosphorylation can only be detected from 0.2 U mL^{-1} thrombin, and is followed by a second phase of LIM domain kinase 1 (LIMK1)-mediated slow cofilin rephosphorylation/inactivation [5]. Regulation of Rac1/LIMK1 by AMPK could explain the significant increase in cofilin phosphorylation that we observed upon thrombin stimulation. Supporting this hypothesis, Rac1 activation downstream of AMPK has already been described in various cell types [26,27]. Very recently, AMPK was shown to activate Tiam-1, a Rac guanine nucleotide exchange factor, in C2C12 cells [28]. As preincubation with STO-609 did not completely abolish the phosphorylation of cytoskeletal targets in human platelets, we cannot exclude the possibility that AMPK-independent pathways might also play a role in this regulation.

AMPK has also been recognized as a VASP kinase responsible for Thr278 and Ser322 phosphorylation [9,13]. VASP phosphorylation regulates VASP-driven actin filament formation and subcellular targeting of the protein *in vivo* [8]. In this regard, AMPK-mediated VASP phosphorylation on Thr278 and Ser322 interferes with F-actin accumulation, but has a minor impact on subcellular targeting. When platelets are activated, the extension of filopodia is a rapid and transient phenomenon that is quickly superseded by the formation of lamellipodia, resulting in platelet spreading. Phosphorylation and rapid inhibition of VASP anticapping activity by AMPK might be crucial for the regulation of these dynamic structures in an adequate time range. Our results demonstrating that the percentage of platelets showing lamellipodia was significantly reduced in thrombin-stimulated KO platelets, after spreading on fibrinogen-coated coverslips, support this hypothesis. In consequence, it was not surprising to find that this altered cytoskeletal response was associated with slower and less effective clot retraction in KO platelets. However, we have to mention that Randriamboavonjy *et al*. [18] failed to show a significant difference in thrombin-induced clot retraction between platelets from AMPK-α1 KO and WT mice.

Finally, we took advantage of the specific action of thrombin on ACC phosphorylation to demonstrate that the AMPK pathway was activated *in vivo* in platelets from patients undergoing cardiac surgery, a clinical situation associated with thrombin generation. Our preliminary clinical data clearly indicate that ACC phosphorylation is a potential indicator of thrombin response *in vivo*.

In conclusion, we have delineated a CaMKKβ–AMPK-α1-dependent pathway contributing to murine and human platelet aggregation upon thrombin stimulation, via MLC, VASP and cofilin phosphorylation and cytoskeletal reorganization. This pathway is activated in a heparin-sensitive manner in platelets of patients undergoing major cardiac surgery.

Addendum

S. Horman and C. Beauloye designed the study and wrote the paper. M. B. Onselaer performed the experiments. C. Oury, J. L. Vanoverschelde, and L. Bertrand contributed to the analysis and interpretation of data. S. Eeckhoudt participated in aggregation studies on human platelets. C. Lecut helped with the aggregation studies on murine platelets. N. Morel participated in Ca^{2+} measurements. N. Barile and L. M. Jacquet contributed to blood sampling in patients in the ICU.

Acknowledgements

This work was made possible by grants from Fonds National de la Recherche Scientifique (FNRS), Belgium. M.-B. Onselaer was supported by a grant from Fonds Spéciaux de Recherche (FSR), by a Bourse du Patrimoine, Université catholique de Louvain, and by the Salus Sanguinis Foundation, Belgium. S. Horman, L. Bertrand and C. Oury are Research Associates of FNRS, and C. Beauloye is an MD postdoctoral fellow, FNRS, Belgium. We thank N. Marquet for his expert technical assistance.

Disclosure of Conflict of Interests

The authors state that they have no conflict of interest.

Supporting Information

Additional Supporting Information may be found in the online version of this article:

Part S1: Supplemental Materials and Methods.
Part S2: Supplemental data.
Fig. S1. Effect of activating peptides for PAR1 and PAR4 on ACC phosphorylation in human platelets.
Fig. S2. (A) Western blot analysis of CaMKKβ expression in extracts from human platelets. (B) Lack of effect of STO-609 on ACC phosphorylation induced by A-769662 treatment in human platelets.
Fig. S3. Aggregation and ATP secretion analyses.
Fig. S4. (A) Assessment of Ca^{2+} release in response to various agonists in the presence or absence of STO-609. (B) Assessment of TXB_2 levels in platelet supernatants.
Fig. S5. AMPK-α1 regulates thrombin-induced, U46619-induced and collagen-induced ACC phosphorylation in murine platelets.
Fig. S6. Role of AMPK-α1 in murine platelet aggregation and secretion, in response to various agonists.
Fig. S7. Role of AMPK-α1 in thrombin-dependent F-actin formation.

References

1 Jackson SP. The growing complexity of platelet aggregation. *Blood* 2007; **109**: 5087–95.
2 Johnson GJ, Leis LA, Krumwiede MD, White JG. The critical role of myosin IIA in platelet internal contraction. *J Thromb Haemost* 2007; **5**: 1516–29.
3 Fox JE. Regulation of platelet function by the cytoskeleton. *Adv Exp Med Biol* 1993; **344**: 175–85.
4 Getz TM, Dangelmaier CA, Jin J, Daniel JL, Kunapuli SP. Differential phosphorylation of myosin light chain (Thr)18 and (Ser) 19 and functional implications in platelets. *J Thromb Haemost* 2010; **8**: 2283–93.
5 Pandey D, Goyal P, Dwivedi S, Siess W. Unraveling a novel Rac1-mediated signaling pathway that regulates cofilin dephosphorylation and secretion in thrombin-stimulated platelets. *Blood* 2009; **114**: 415–24.
6 Hansen SD, Mullins RD. VASP is a processive actin polymerase that requires monomeric actin for barbed end association. *J Cell Biol* 2010; **191**: 571–84.
7 Pula G, Schuh K, Nakayama K, Nakayama KI, Walter U, Poole AW. PKCdelta regulates collagen-induced platelet aggregation through inhibition of VASP-mediated filopodia formation. *Blood* 2006; **108**: 4035–44.
8 Benz PM, Blume C, Seifert S, Wilhelm S, Waschke J, Schuh K, Gertler F, Munzel T, Renne T. Differential VASP phosphorylation controls remodeling of the actin cytoskeleton. *J Cell Sci* 2009; **122**: 3954–65.
9 Thomson DM, Ascione MP, Grange J, Nelson C, Hansen MD. Phosphorylation of VASP by AMPK alters actin binding and occurs at a novel site. *Biochem Biophys Res Commun* 2011; **414**: 215–19.
10 Stahmann N, Woods A, Carling D, Heller R. Thrombin activates AMP-activated protein kinase in endothelial cells via a pathway involving Ca^{2+}/calmodulin-dependent protein kinase kinase beta. *Mol Cell Biol* 2006; **26**: 5933–45.
11 Witters LA, Kemp BE, Means AR. Chutes and ladders: the search for protein kinases that act on AMPK. *Trends Biochem Sci* 2006; **31**: 13–16.
12 Miranda L, Carpentier S, Platek A, Hussain N, Gueuning MA, Vertommen D, Ozkan Y, Sid B, Hue L, Courtoy PJ, Rider MH, Horman S. AMP-activated protein kinase induces actin cytoskeleton reorganization in epithelial cells. *Biochem Biophys Res Commun* 2010; **396**: 656–61.
13 Blume C, Benz PM, Walter U, Ha J, Kemp BE, Renne T. AMP-activated protein kinase impairs endothelial actin cytoskeleton assembly by phosphorylating vasodilator-stimulated phosphoprotein. *J Biol Chem* 2007; **282**: 4601–12.
14 Horman S, Morel N, Vertommen D, Hussain N, Neumann D, Beauloye C, El Najjar N, Forcet C, Viollet B, Walsh MP, Hue L, Rider MH. AMP-activated protein kinase phosphorylates and desensitizes smooth muscle myosin light chain kinase. *J Biol Chem* 2008; **283**: 18505–12.
15 Jorgensen SB, Viollet B, Andreelli F, Frosig C, Birk JB, Schjerling P, Vaulont S, Richter EA, Wojtaszewski JF. Knockout of the alpha2 but not alpha1 5′-AMP-activated protein kinase isoform abolishes 5-aminoimidazole-4-carboxamide-1-beta-4-ribofuranoside but not contraction-induced glucose uptake in skeletal muscle. *J Biol Chem* 2004; **279**: 1070–9.
16 Sakamoto K, Goransson O, Hardie DG, Alessi DR. Activity of LKB1 and AMPK-related kinases in skeletal muscle: effects of contraction, phenformin, and AICAR. *Am J Physiol Endocrinol Metab* 2004; **287**: E310–17.
17 Rowley JW, Oler AJ, Tolley ND, Hunter BN, Low EN, Nix DA, Yost CC, Zimmerman GA, Weyrich AS. Genome-wide RNA-seq analysis of human and mouse platelet transcriptomes. *Blood* 2011; **118**: e101–11.
18 Randriamboavonjy V, Isaak J, Fromel T, Viollet B, Fisslthaler B, Preissner KT, Fleming I. AMPK alpha2 subunit is involved in platelet signaling, clot retraction, and thrombus stability. *Blood* 2010; **116**: 2134–40.
19 Coughlin SR. Protease-activated receptors in hemostasis, thrombosis and vascular biology. *J Thromb Haemost* 2005; **3**: 1800–14.
20 Spalton JC, Mori J, Pollitt AY, Hughes CE, Eble JA, Watson SP. The novel Syk inhibitor R406 reveals mechanistic differences in the initiation of GPVI and CLEC-2 signaling in platelets. *J Thromb Haemost* 2009; **7**: 1192–9.
21 Xiang B, Zhang G, Stefanini L, Bergmeier W, Gartner TK, Whiteheart SW, Li Z. The Src family kinases and protein kinase C synergize to mediate Gq-dependent platelet activation. *J Biol Chem* 2012; **287**: 41277–87.
22 Green MF, Scott JW, Steel R, Oakhill JS, Kemp BE, Means AR. Ca^{2+}/calmodulin-dependent protein kinase kinase beta is regulated by multisite phosphorylation. *J Biol Chem* 2011; **286**: 28066–79.
23 Kawano Y, Fukata Y, Oshiro N, Amano M, Nakamura T, Ito M, Matsumura F, Inagaki M, Kaibuchi K. Phosphorylation of myosin-binding subunit (MBS) of myosin phosphatase by Rho-kinase in vivo. *J Cell Biol* 1999; **147**: 1023–38.
24 Banko MR, Allen JJ, Schaffer BE, Wilker EW, Tsou P, White JL, Villen J, Wang B, Kim SR, Sakamoto K, Gygi SP, Cantley LC, Yaffe MB, Shokat KM, Brunet A. Chemical genetic screen for AMPKalpha2 substrates uncovers a network of proteins involved in mitosis. *Mol Cell* 2011; **44**: 878–92.
25 Aslan JE, McCarty OJ. Rho GTPases in platelet function. *J Thromb Haemost* 2013; **11**: 35–46.
26 Lee YM, Lee JO, Jung JH, Kim JH, Park SH, Park JM, Kim EK, Suh PG, Kim HS. Retinoic acid leads to cytoskeletal rearrangement through AMPK-Rac1 and stimulates glucose uptake

through AMPK-p38 MAPK in skeletal muscle cells. *J Biol Chem* 2008; **283**: 33969–74.

27 Bae HB, Zmijewski JW, Deshane JS, Tadie JM, Chaplin DD, Takashima S, Abraham E. AMP-activated protein kinase enhances the phagocytic ability of macrophages and neutrophils. *FASEB J* 2011; **25**: 4358–68.

28 You GY, Lee JO, Kim JH, Kim N, Lee SK, Moon JW, Jie S, Lee HJ, Kim SJ, Park SH, Kim HS. Tiam-1, a GEF for Rac1, plays a critical role in metformin-mediated glucose uptake in C2C12 cells. *Cell Signal* 2013; **12**: 2558–65.